

Design and Fabrication of an Electrostatic Variable Gap Comb Drive in Micro-Electro-Mechanical Systems

Wenjing Ye¹, Subrata Mukherjee²

Abstract: Polynomial driving-force comb drives are designed using numerical simulation. The electrode shapes are obtained using the indirect boundary element method. Variable gap comb drives that produce combinations of linear, quadratic, and cubic driving-force profiles are synthesized. This inverse problem is solved by an optimization procedure. Sensitivity analysis is carried out by the direct differentiation approach (DDA) in order to compute design sensitivity coefficients (DSCs) of force profiles with respect to parameters that define the shapes of the fingers of a comb drive. The DSCs are then used to drive iterative optimization procedures. Designs of variable gap comb drives with linear, quadratic and cubic driving force profiles are presented in this paper. Based on these designs, a comb drive which produces cubic polynomial driving force has been fabricated using the SCREAM I process. Test results show reasonable agreement between numerical simulations and experiments.

keyword: optimal design, boundary element method, micro-electro-mechanical systems, comb drive

1 Introduction

Micro-electro-mechanical (MEM) devices are integrated, movable microstructures with electronics. These miniaturized mechanical systems offer unique opportunities for scientific breakthroughs and technological innovations, and are on the verge of starting an entirely new industry. During the past decade, the growth of new process technologies and new device concepts in the field of MEMS has been phenomenal. Applications of MEMS can be found in many areas. According to 1994 System Planning Corporation MEMS market study, in the year 2000, the MEMS market will reach nearly 90 billion dollars.

An electrostatic comb-drive actuator, consisting of interdigitated capacitors, is one of the most important of MEM devices. Electrostatic combs have been used for static actuation of friction test structures [Lim, Chang, Schultz, Howe, and White (1990)], microgrippers [Kim, Pisano, Muller, and lim (1990)], force balanced accelerometers [Yun, Howe, and Gray (1992)] and resonant structures [Pisano (1989)].

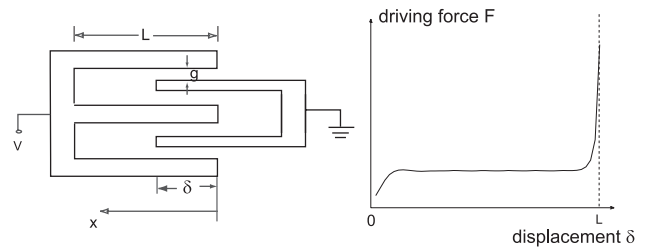


Figure 1 : A standard comb drive and its force profile.

In a typical comb drive, the gap between the fixed and moving fingers is uniform, resulting in an electrostatic driving force which is independent of the position of the moving fingers except at the ends of the range of travel (Fig. 1). It is possible, by changing this gap profile, to obtain different force profiles. It is of interest in some applications to have force profiles such as linear, quadratic or cubic. One example is that, in many actuator applications, large displacement motion is highly desirable. However, the actuator springs exhibit nonlinear response for large displacements. The spring restoring force behaves as $R = k_1x + k_2x^3 + \dots$, where x is the displacement and k_i are the spring constants. A large driving force is required in order to overcome the nonlinear restoring forces. Hence, a prohibitively large voltage must be applied on conventional comb actuators in order to achieve a large range of motion. It is therefore desirable to have comb drives with changing gap profiles such that the corresponding driving force profiles have similar nonlinear terms in x as does the restoring force, for a given applied voltage. Another example is related to tuning MEMS. A comb drive with linear, quadratic or cubic force profile can be used for electrostatic tuning. In many MEMS applications, micromechanical resonators play an important role. In such devices, independent tuning of linear or nonlinear stiffness coefficients is an important issue [Adams (1996)], especially in a device which has large displacement motions. Fig. 2 shows a schematic picture of a tunable resonant structure using variable comb drives (C). The polynomial force (linear or cubic) produced by the variable comb drives can be used to counteract the linear or cubic restoring forces of the beams (B). Optimal shape design of such comb drives has been presented in Ye, Mukherjee, and MacDonald (1998).

There are many MEMS simulation tools available in the lit-

¹ Georgia Institute of Technology, School of Mechanical Engineering, 281 Ferst Drive, SSTC #1, Room 209, Atlanta, GA 30332-0405

² Department of Theoretical and Applied Mechanics, Kimball Hall, Cornell University, Ithaca, NY 14853

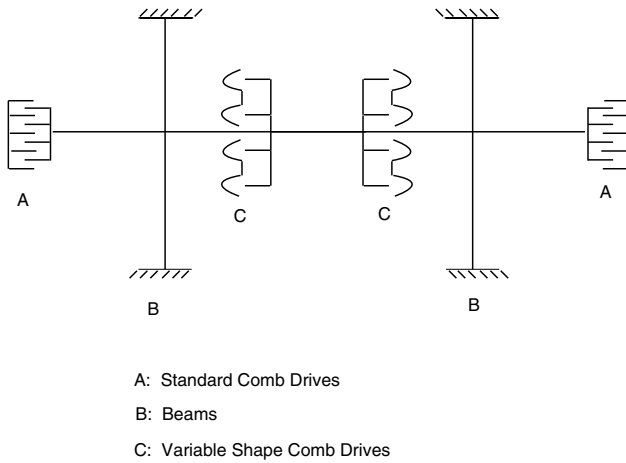


Figure 2 : A schematic picture of a tunable resonant structure.

erature. Among them, MEMCAD from Microcosm Technology Inc. is an integrated package for mask layout, fabrication process description, geometric modeling, electro-mechanical simulation, and results visualization [Senturia (1995)]. It incorporates custom tools for mask layout, and for capacitance calculation using a BEM code (called FASTCAP). Standard commercial packages are used for geometric modeling (SDRC's IDEAS) and structural analysis (ABAQUS). It also has CoSolve-EM for self-consistent coupled-domain electromechanical analysis. Some work based on MEMCAD has already been reported recently [Gilbert, Ananthasuresh, and Senturia (1996)]. Another commercially available package is IntelliCAD from IntelliSense Corp. (<http://www.intellis.com>) which includes both commercial and custom tools and databases [He, Harris, Napadenski, and Maseeh (1996)]. IntelliSense software products are also directed at providing MEMS modeling and simulation capability. However, these commercial CAD systems applicable to MEMS are primarily aimed at simulation and fabrication processes and electro-mechanical behavior of a given design. Parametric optimization of a design for specified requirements is not feasible except by iterating the simulation over many input data sets - which is computationally expensive and time consuming.

The present review paper addresses the issues of simulation, design (inverse problem) and fabrication of comb drives with variable gap profiles. Two-dimensional simulations of the exterior electrostatic field, and the resultant forces on the comb drive, are carried out with the exterior, indirect, boundary element method. Following direct simulation, sensitivity analysis is carried out by the direct differentiation approach (DDA) [Haug, Choi, and Komkov (1986)]. The variable of interest is the driving force while the design variables are parameters that determine the shape of the fixed fingers. (Initially, the widths of the moving fingers are assumed to remain uniform). Next, an inverse problem is posed as follows: determine the width

profile of the fixed fingers (and hence the gap profile) such that the driving force is a desired function of the displacement of the comb drive. Linear, quadratic and cubic functions are considered in this work. The optimization code "dlcong" from the IMSL package (User's Manual) is used for this phase of the work.

It is found that designs with uniform width moving fingers have certain shortcomings including a large size. An improved design is proposed in which both the fixed and moving fingers have variable width. This design reduces the size of the device almost by half, but by comparing with the standard comb drive, it is still quite large. A different approach based on changing the height profile of the comb has been used to design comb drives to have variable force profiles [Ye and Mukherjee (1999)]. This design preserves the original size, but is difficult to fabricate with present day MEMS technology.

A cubic comb drive based on the improved design has been fabricated using the Single Crystal Reactive Etching And Metallization (SCREAM) I process [Shaw, Zhang, and MacDonald (1994)]. The electrical test results indicate that this design is more stable than comb drives with uniform gap profiles, and the measured driving force agrees reasonably well with the simulation result.

2 Mathematical formulation

2.1 The driving force on a comb drive

An ideal comb drive can be modeled as a system of m conductors embedded in a uniform lossless dielectric medium (see Fig. 3). Each conductor has a constant electrostatic potential. The charge on each conductor is distributed on its surface and satisfies the Eq. 1 [Jackson (1975)]:

$$q_i(\mathbf{r}) = \epsilon \frac{\partial \phi_i(\mathbf{r})}{\partial \mathbf{n}} \quad (1)$$

where $q_i(\mathbf{r})$ is the surface charge density at point \mathbf{r} on the surface of conductor i , ϵ is the dielectric constant of the medium, ϕ_i is the electrostatic potential of conductor i and \mathbf{n} is the inward normal to a conductor at point \mathbf{r} .

The electrostatic potential ϕ in the region exterior to the conductors satisfies the Laplace equation:

$$\nabla^2 \phi = 0 \quad (2)$$

with the boundary conditions: $\phi = \phi_i$ on conductor i , $i = 1, 2, \dots, m$, where m is the total number of conductors.

Using the indirect boundary element method formulation proposed by Shi, Ramesh, and Mukherjee (1995), the surface charge density $q_i(\mathbf{r})$ on conductor i can be obtained by solving the following Eq. 3, and Eq. 4 together with Eq. 1:

$$\phi_i = \sum_{j=1}^m \int_{\partial s_j} \frac{\partial \phi}{\partial \mathbf{n}}(\mathbf{r}') G(\mathbf{r}, \mathbf{r}') ds(\mathbf{r}') + \hat{C} \quad (3)$$

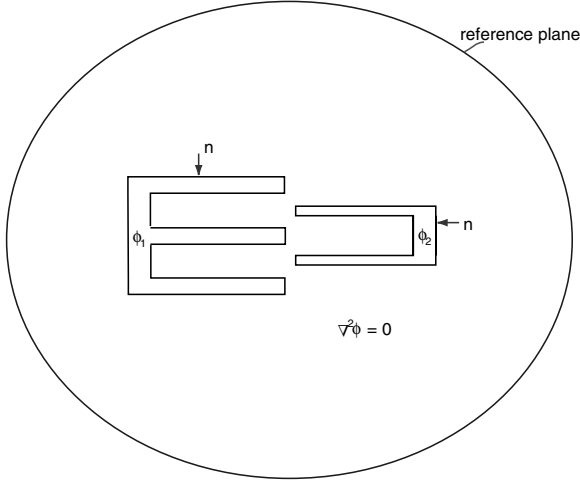


Figure 3 : A system of m -ideal conductors embedded in a uniform lossless dielectric medium.

$$Q = \sum_{j=1}^m \int_{\partial s_j} \frac{\partial \phi}{\partial n}(\mathbf{r}') ds(\mathbf{r}') \quad (4)$$

where \mathbf{r} is the position vector of source point, \mathbf{r}' is the position vector of field point, G is the Green's function, (which is equal to $\frac{1}{2\pi} \ln \|\mathbf{r} - \mathbf{r}'\|$ in 2-D, $\frac{1}{4\pi \|\mathbf{r} - \mathbf{r}'\|}$ in 3-D), ∂s_j is the surface of conductor j , Q is the total charge of the system, which is 0 in this work, and \hat{C} is a constant.

The relationship between the electrostatic force f acting on the surface of a conductor and the charge density q of that conductor is:

$$\mathbf{f} = -\frac{1}{2} \frac{q^2}{\epsilon} \mathbf{n} \quad (5)$$

Thus, the driving force acting on the moving fingers along travel (x) direction

$$F = \int_{\Gamma} f_x ds \quad (6)$$

can be calculated from Eq. 5 if q is known. Here, f_x is the x component of force \mathbf{f} and Γ is the surface of the moving fingers.

2.2 Sensitivity Analysis

Design sensitivity coefficients (DSCs) are the derivatives of physical quantities, for example force, stress, temperature etc., with respect to design variables such as geometrical parameters that determine the shape of a structure. In optimization problems, they are used as a guide to the best search direction in nonlinear programming algorithms. These algorithms typically iterate on the design variables along these directions until an optimal design is obtained. Accurate determination of the

DSCs typically leads to fast convergence, and thus to more efficient design. There are several methods for computing DSCs. Among them, the finite difference method (FDM) is the easiest one. It calculates two functions from two slightly different design variables, and takes the difference of these functions divided by the difference of the design variables, as the DSC. This method is very easy to use but may not be accurate. In the present work, the direct differentiation approach (DDA) is used to find the design sensitivity coefficients. DSCs are calculated by differentiating Eq. 3 and Eq. 4 with respect to design variables and solving the resultant equations. One of the advantages of the DDA is high accuracy. The computed DSCs are typically obtained with the same accuracy as the physical quantities. The other advantage is computing efficiency. After discretizing the resultant integral equations, the linear system obtained has the same coefficient matrix A as the one obtained for the calculation of the physical quantities. Only the right hand side vector b must be recalculated.

In this work, the design variables are the shape parameters of a comb drive and the physical quantity is the driving force acting on the moving finger.

2.2.1 Gradients

Let c be one of the parameters that determine the shape of a finger (fixed or moving) of a comb drive. The precise shape parameters, used in this work, are defined later. From Eq. 6, the gradient of the driving force F with respect to c is

$$\dot{F} = \int_{\Gamma} \dot{f}_x ds + \int_{\Gamma} f_x \dot{ds} \quad (7)$$

where $\dot{(\cdot)} = \frac{\partial}{\partial c}$.

From Eq. 5, the sensitivity of f_x is

$$\dot{f}_x = -\frac{q \dot{q}}{\epsilon} n_x - \frac{1}{2} \frac{q^2}{\epsilon} \dot{n}_x \quad (8)$$

Please refer to, for example, Chandra and Mukherjee (1997) for formulae for \dot{ds} and \dot{n}_x .

The sensitivity of the charge density q can be obtained by solving the following equations:

$$\begin{aligned} \sum_{j=1}^n \int_{\partial s_j} \dot{q}(\mathbf{r}') G(\mathbf{r}, \mathbf{r}') ds(\mathbf{r}') + \dot{C} = \\ - \sum_{j=1}^n \int_{\partial s_j} q(\mathbf{r}') \dot{G}(\mathbf{r}, \mathbf{r}') ds(\mathbf{r}') \\ - \sum_{j=1}^n \int_{\partial s_j} q(\mathbf{r}') G(\mathbf{r}, \mathbf{r}') \dot{ds}(\mathbf{r}') \end{aligned} \quad (9)$$

$$\sum_{j=1}^n \int_{\partial s_j} \dot{q}(\mathbf{r}') ds(\mathbf{r}') = - \sum_{j=1}^n \int_{\partial s_j} q(\mathbf{r}') \dot{ds}(\mathbf{r}') \quad (10)$$

Here, $C = \epsilon \hat{C}$ is a constant.

Eq. 9 and Eq. 10 are obtained by differentiating Eq. 3 and Eq. 4 with respect to c .

2.3 The inverse problem

The design of a variable comb drive, with linear, quadratic or cubic driving force, can be posed as an optimal design problem. The goal of the optimization procedure is to minimize an objective function without violating the specified constraints.

The optimization problem is set up as

$$\min \psi(c_i)$$

subject to the constraints: $a_i(c_j) \leq 0$

where the objective function ψ is chosen as the integral of the square of the difference between the actual and desired force profiles, over the range of operation of the comb drive, i.e.:

$$\psi(c_i) = \int_{\ell_1}^{\ell_2} (F(c_i, x) - F_e(x))^2 dx \quad (11)$$

Here, c_i are the shape parameters of the comb drive, F is the driving force, x is the position of a moving finger, $F_e(x)$ is the desired force profile that can be linear, quadratic or cubic (such as the driving force needed to counteract the cubic restoring force of nonlinear actuator springs), ℓ_1, ℓ_2 are the initial and final positions of a moving finger and a_i are the constraints imposed by practical design issues, such as the minimum gap between fingers, etc.

The sensitivity of the objective function ψ with respect to a design variable c is

$$\Psi = \int_{\ell_1}^{\ell_2} 2(F(c_i, x) - F_e(x)) F dx \quad (12)$$

The design methodology adopted in this work is outlined in Fig. 4. Simulation and sensitivity analysis are carried out for an initial design. This information is supplied to an optimizer which produces a better design - one that reduces the value of the objective function without violating the constraints of the problem. Iterative improvements in designs continue until a preset stopping criterion is satisfied. This is the final design.

3 Numerical implementation and examples

3.1 The driving force

A prototype comb drive with one set of straight fingers is considered here. (see Fig. 5). The surface charge density q on the comb drive is calculated from Eq. 3 and Eq. 4 using the boundary element method. In order to avoid the singularities, the corners are “rounded off” by Hermitian curves.

Numerical results for the driving force as a function of the distance traveled by the moving finger are shown in Fig. 5. Also, the results from an approximate formula, which is widely used

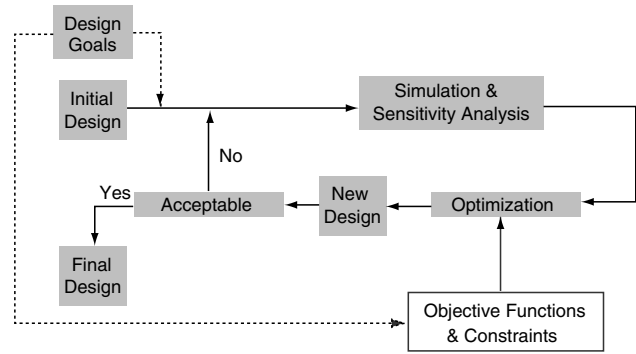


Figure 4 : Flow chart for optimal design.

in practice, are shown there for comparison. This formula, based on a capacitance model [McMillan (1993)], is:

$$F = \epsilon \frac{hV^2}{g} \quad (13)$$

where F is the driving force acting on a moving finger, h is the height of the finger (in a direction normal to Fig. 5), and V and g are the bias voltage and the gap between the fixed and moving fingers, respectively. The results show that the driving force remains constant if the gap g and the height h remain constant. The difference between the two solutions is only 1.1 percent.

3.2 Sensitivity Analysis

3.2.1 Design variables

It is assumed that the fixed fingers of a comb drive are of variable width while the moving fingers are uniform. In view of the approximate formula (13), it is proposed that the gap profile between a fixed and a moving finger be an inverse polynomial

$$g(x) = \frac{1}{c_0 + c_1x + c_2x^2 + c_3x^3} \quad (14)$$

where $c_i, i = 0, 1, 2, 3$ are the design variables. All the sensitivities of the physical quantities are calculated with respect to c_i .

3.2.2 Gradients

Numerical results for $\partial q / \partial c_i$ from the DDA of the BEM, are compared with those computed by the finite difference method (FDM) in Fig. 6. Suitable choice of perturbations in the design variables ($\Delta c_0 = 0.01, \Delta c_1 = 0.001, \Delta c_2 = 0.0001, \Delta c_3 = 0.00001$) leads to very good agreement between the results from the two methods, when the gradients are not very large. When the value of q is very sensitive to those of c_i , bigger discrepancies between the results are observed. However, the forces in this problem are mostly determined by the fringe field

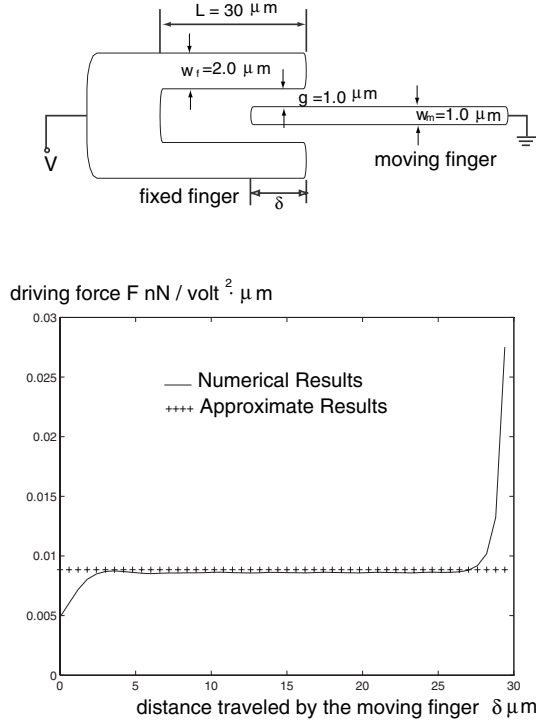


Figure 5 : A prototype comb drive with one set of straight fingers and its force profile.

so that the values of the sensitivities on the tip of the moving finger (nodes 105 - 115) are of primary interest. In this region, the results from the DDA and the FDM agree.

One can also calculate the sensitivity of the maximum driving force (F_{max}) (when the moving fingers are fully inserted) with respect to the gap profile. For example, one can pick a specific point, the corner point on the fixed finger (which corresponds to the first spike in Fig. 6), and calculate the quantity $\frac{|\Delta F|/F}{|\Delta g|/g}$, keeping the slope g' and curvature g'' of g constant at that point. This has been done and the result is

$$\frac{|\Delta F|/F}{|\Delta g|/g} = 0.7869 \quad (15)$$

Similarly, one can find the quantity $\frac{|\Delta F|/F}{|\Delta g''|/g''}$, keeping the gap g and slope g' constant at that point. This time, one gets

$$\frac{|\Delta F|/F}{|\Delta g''|/g''} = 0.146 \quad (16)$$

3.3 The inverse problem

The goal here is to design three variable comb-drives which have linear, quadratic or cubic driving force profiles as functions of the distance traveled by the movable finger. However, a comb drive with purely linear, quadratic or cubic driving

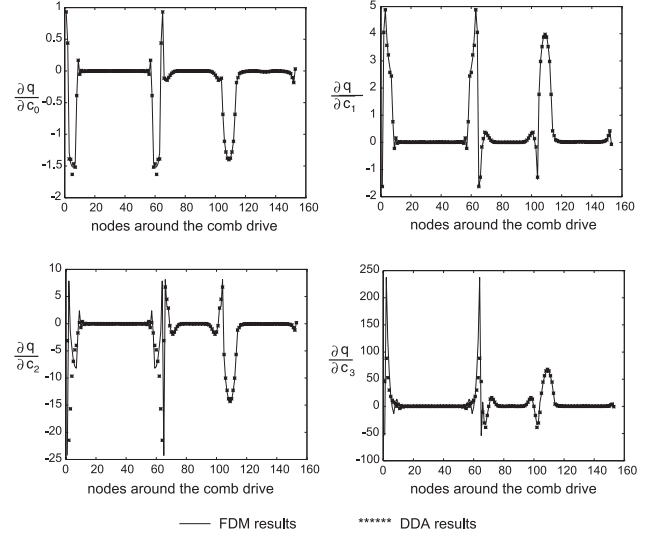


Figure 6 : Numerical results for the sensitivities of charge density with respect to shape parameters.

force profile usually occupies a large area. For example, for a comb drive with driving force $F(x) = cx^3$, according to the simple formula (13), the gap $g(x)$ will be roughly proportional to $\frac{1}{x^3}$. If x , the position of the tip of the moving finger, varies between $5\mu\text{m}$ to $25\mu\text{m}$, the gaps at the two ends will have a ratio of 125, i.e. if $g(x)$ at $x = 25\mu\text{m}$ is $1\mu\text{m}$, then $g(x)$ at $x = 5\mu\text{m}$ will be $125\mu\text{m}$! This will result in an unacceptably wide comb drive. Due to this practical design consideration, the range of x in the desired function $h(x)$ is shifted by x_0 . Instead of having $h(x)$ proportional to x , x^2 , or x^3 , it is taken to be proportional to $x + x_0$, $(x + x_0)^2$ or $(x + x_0)^3$. By choosing suitable values of x_0 , the opening between the fixed fingers can be controlled. Also, in these examples, the design space is enlarged by adding another term, c_4x^4 , in the denominator of the expression for $g(x)$ in Eq. 14.

The new objective function ψ for the inverse problem is:

$$\psi(c_i) = \int_{\ell_1}^{\ell_2} (F(c_i, x) - F_e(x + x_0))^2 dx \quad (17)$$

This problem has been solved by using the optimization code “dlcong” from the IMSL package. This code is based on M.J.D. Powell’s TOLMIN, which solves linearly constrained optimization problems. The optimizer uses the function F and sensitivity F' (Eq. 6, 7) from the comb drive simulations that have been presented in this paper. The second derivatives are approximated in “dlcong” by the BFGS formula, developed by Brodyen, Fletcher, Goldfrab and Shanno.

Three designs are shown in Fig. 7, along with their force profiles. The final design for the linear comb drive was obtained after 10 iterations. The final designs for the quadratic and cubic comb drives were obtained after 15 iterations. However,

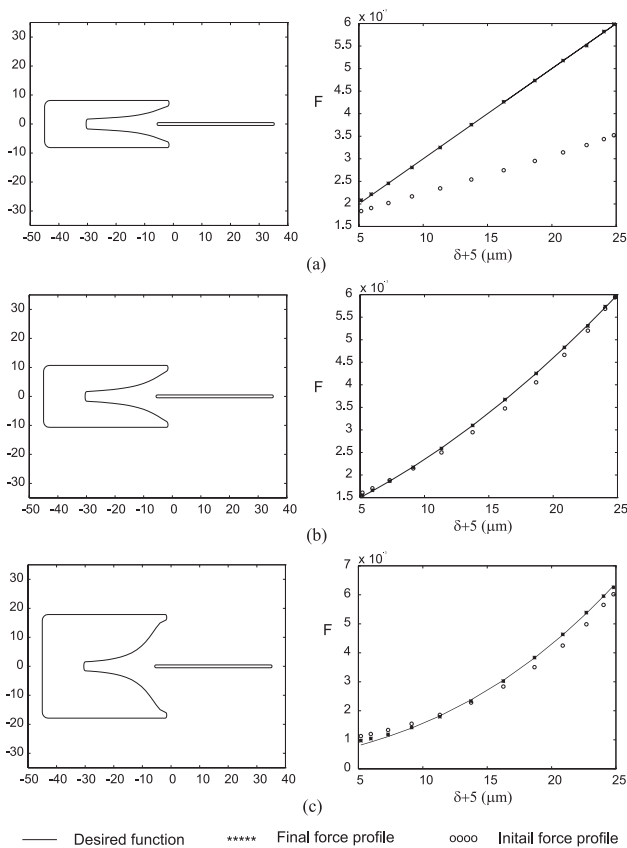


Figure 7 : Designs of variable comb drives with uniform moving fingers, together with their force profiles. (a) linear motor, (b) quadratic motor, (c) cubic motor.

in these designs, the driving forces they produce are relatively small at the maximum gap, especially for the cubic motor. In order to overcome this drawback, the moving finger is also shaped. The shape of the moving finger is chosen such that when it is fully inserted, the gap profile becomes uniform. The resultant comb drives have several advantages. First, the maximum driving force increases dramatically, especially for the cubic motor. Second, the structure is more stable and therefore large voltages can be applied. Finally, the area occupied by a comb drive is much smaller. The new designs with variable widths of both the fixed and the moving fingers, and their force profiles, are shown in Fig. 8. Tab. 1 gives a comparison of a straight standard comb drive with the two kinds of variable shape. The minimum gap in each comb drive is $1.5\mu\text{m}$ and the maximum displacement of the moving fingers is $20\mu\text{m}$. These fundamental comb drives can be arranged in parallel, with suitable bias voltages applied to each comb drive, in order to obtain any desired polynomial (up to cubic) force profile.

Table 1 : Force ranges of different comb drives

	force profile	force range (nN / volt ² × μm)
Standard comb drive	Constant	0.0059
Comb drive with uniform moving fingers	Linear	(0.002, 0.006)
	Quadratic	(0.0015, 0.006)
	Cubic	(0.0010, 0.0063)
Comb drive with variable moving finger	Linear	(0.0042, 0.011)
	Quadratic	(0.0033, 0.014)
	Cubic	(0.0023, 0.013)

4 Fabrication

A cubic comb drive based on the design in Fig. 8c was fabricated using SCREAM I process. SCREAM I is a single mask bulk micromachining process. It uses Reactive Iron Etch (RIE) of a silicon substrate to fabricate suspended movable single-crystal silicon structures. Only one lithography step is needed to define beams and structures simultaneously as well as all necessary contact pads, electrical interconnects and lateral capacitors. A brief outline of the SCREAM I process is described in Fig. 9, 10, and 11.

All the process steps were operated at low temperature (< 300°C), and only conventional silicon fabrication tools were used.

Due to limitations of the SCREAM process, the moving fingers in the comb drive were approximated by honey-comb structures (see Fig. 12). The minimum feature size in these stepped shaped fingers was $0.5\mu\text{m}$, while the maximum feature size was $1\mu\text{m}$. The effect of the shape approximation on the driving force was studied by performing a simulation on the honey-comb structure. Fig. 13 shows the comparison of the driving force profiles between the honey-comb structure and the smooth-shaped structure shown in Fig. 8c. The maximum difference is about 10%. The CAD design of the whole device is indicated in Fig. 14.

Fig. 15 shows part of a released structure with one standard comb drive and one variable comb drive. The height of the released structure was about $10\mu\text{m}$.

The device was electrically tested by applying a bias DC voltage to the fixed fingers (the moving fingers were grounded). In the standard comb drive, the moving fingers started to move towards the fixed fingers when the bias voltage was 6 volts. At $V = 14$ volts, the device started to have sideways motion and became unstable. In the variable comb drive, the moving fingers started to move at $V = 5$ volts. Up to 19 volts, the variable comb drive was stable.

The displacements of the moving fingers in the variable comb drive, driven by different voltages, were measured using an

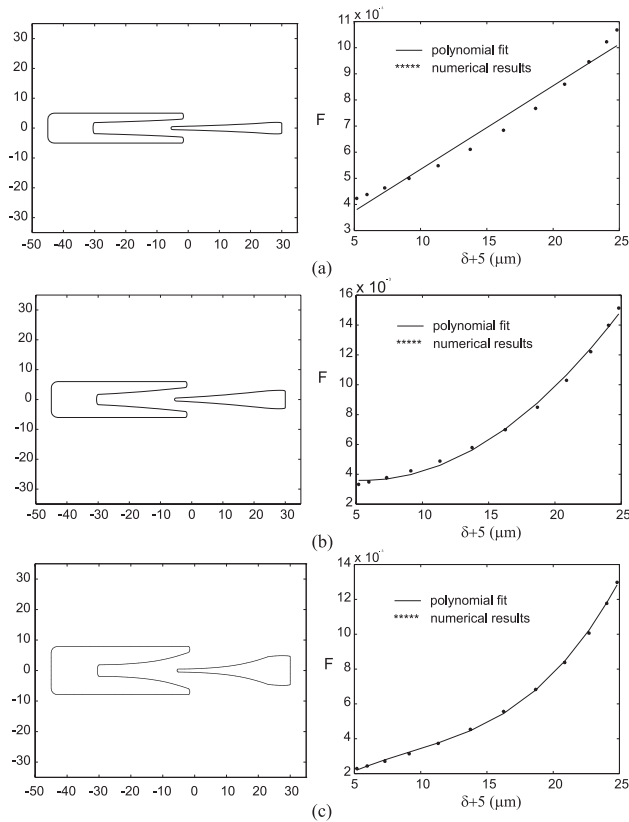


Figure 8 : Designs of variable comb drives with variable moving fingers, together with their force profiles. (a) linear motor: $F(\delta) = 0.00032\delta + 0.0038 \text{ nN/volt}^2 \mu\text{m}$, (b) quadratic motor: $F(\delta) = 3.0 \times 10^{-5}\delta^2 - 3.20 \times 10^{-5}\delta + 0.0036 \text{ nN/volt}^2 \mu\text{m}$, (c) cubic motor: $F(\delta) = 1.57 \times 10^{-6}\delta^3 - 2.00 \times 10^{-5}\delta^2 + 3.2 \times 10^{-4}\delta + 2.14 \times 10^{-3} \text{ nN/volt}^2 \mu\text{m}$.

optical microscope at $\delta = 5\mu\text{m}$. Here δ is the overlap between the fixed and the moving fingers. The driving forces from the comb drive at this configuration were then calculated from the measured displacements. The experimental result is shown in Tab. 2, together with the simulation result from the design in Fig. 8c. The experimental result is the average from three applied voltages - 5, 10, and 15 volts, respectively. The difference between the experimental and the computed results is about 23 %. Further experiments to measure driving forces at different overlap lengths are planned in the future.

5 Conclusions

A comb actuator is a basic actuation device of MEMS. The range of operation of an usual comb drive is limited by its nonlinear restoring spring force. It is shown in this paper that comb drives with variable gap profiles can be designed and fabricated that deliver desired driving force profiles. In principle, therefore, nonlinear (e.g. cubic) spring forces can be can-

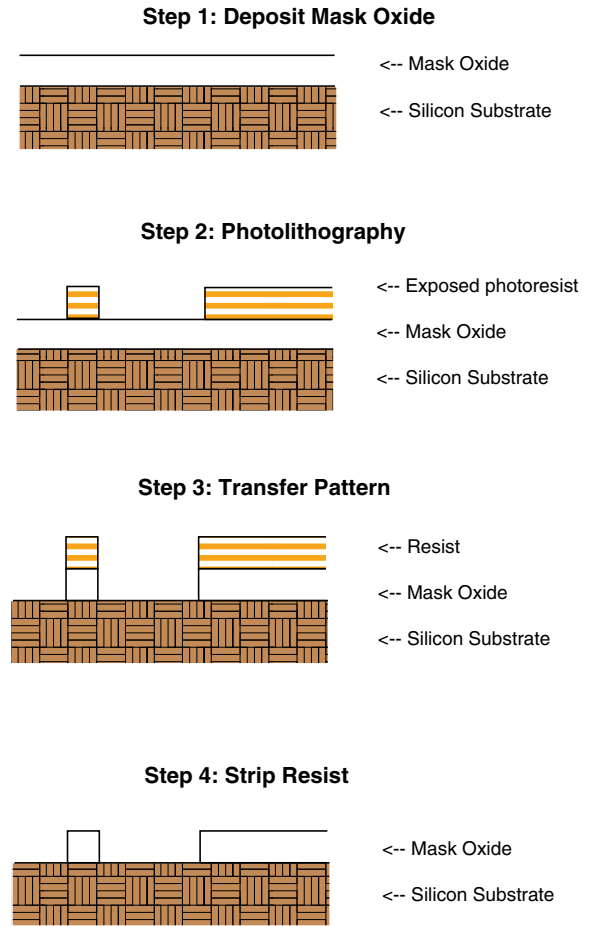


Figure 9 : SCREAM I process outline (reprint from Shaw, Zhang, and MacDonald (1994), part I)

celled by appropriate nonlinear driving forces, thereby greatly increasing the range of operation of a comb actuator. Also, tuning of the linear or nonlinear stiffness coefficients can be carried out conveniently with shape motors.

Transverse stability of the actuator-suspension structure is another important issue in comb drive design. The designs proposed in Fig. 8 are more stable than standard comb drives. Formal inclusion of stability criteria in the optimal design process is recommended for future research.

Acknowledgement: This research has been supported by grant number ECS-9321508 of the US National Science Foundation to Cornell University. The computing for this Research was carried out using the resources of the Cornell Theory Center, which receives funding from Cornell University, New York State, the National Center for Research Resources at the National Institutes of Health, the National Science Foundation, the Defense Department Modernization Program, the United States Department of Agriculture, and corporate partners. The

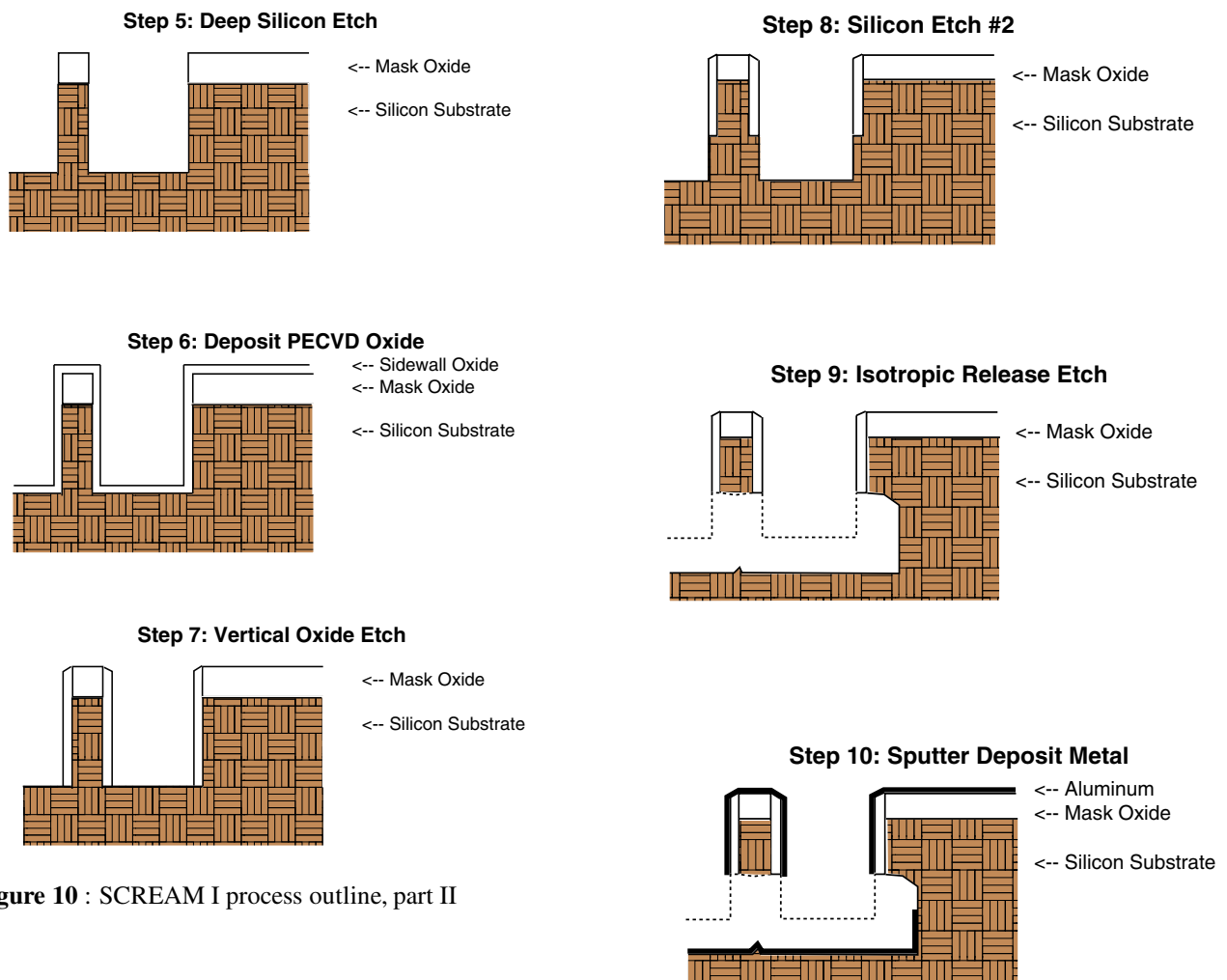


Figure 10 : SCREAM I process outline, part II

Figure 11 : SCREAM I process outline, part III

fabrication of the comb drive was carried out at the Cornell Nanofabrication Facility. Sincere thanks are expressed to Dr. Taher Saif (Mechanical Engineering at the University of Illinois at Urbana Champaign), Dr. Srikanth Kannapan (IBM, Bangalore, India) and Prof. Nick Trefthen (Oxford University, UK) for their many excellent suggestions during the course of this work.

References

Adams, S. (1996): *Design of electrostatic actuators to tune the effective stiffness of micro-electro-mechanical systems*. Ph.D. Thesis, Cornell University.

Chandra, A.; Mukherjee, S. (1997): *Boundary Element Methods in Manufacturing*. Oxford University Press, Oxford, UK.

Gilbert, J. R.; Ananthasuresh, G. K.; Senturia, S. D. (1996): 3D modeling of contact problems and hysteresis in coupled electro-mechanics. In *Proc. IEEE the ninth Annual International Workshop on Micro Electro Mechanical Systems*, pp. 127–132.

Haug, E. J.; Choi, K. K.; Komkov, V. (1986): *Design Sensitivity Analysis of Structural Systems*. Academic Press, New York.

He, Y.; Harris, R.; Napadenski, G.; Maseeh, F. (1996): A virtual prototype manufacturing software system for MEMS.

Table 2 : Driving force from the variable comb drive shown in Fig. 8c

	driving force per finger (nN / volt ² × μm)
experimental result	1.729 × 10 ⁻³
simulation result	2.25 × 10 ⁻³

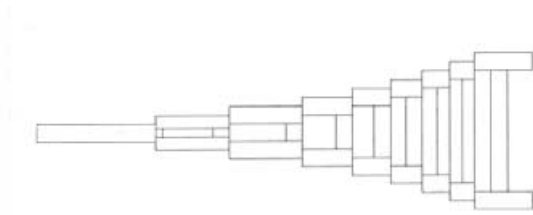
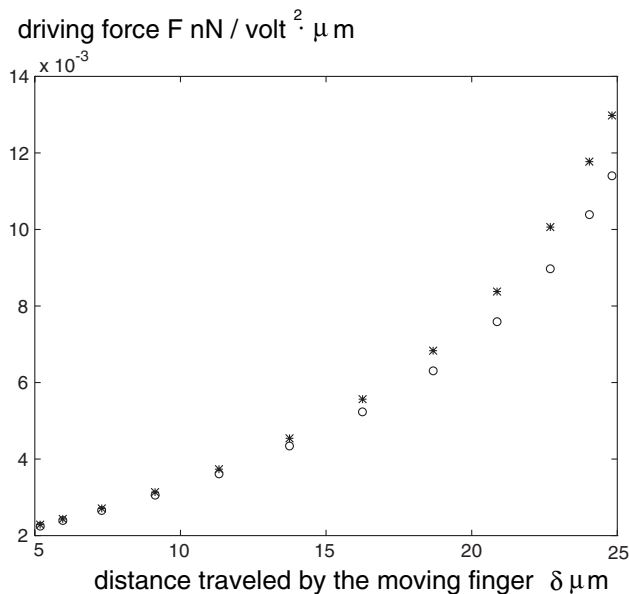


Figure 12 : CAD design of the moving finger in a variable comb drive.



"***" driving force from the cubic motor

"ooo" driving force from the approximate motor

Figure 13 : Driving force profiles from the approximate comb drive and the ideal cubic motor.

In *Proc. IEEE the ninth Annual International Workshop on Micro Electro Mechanical Systems*, pp. 122–126.

Jackson, J. D. (1975): *Classical Electrodynamics, Second Edition*. Wiley, Singapore.

Kim, C. J.; Pisano, A. P.; Muller, R. S.; lim, M. G. (1990): Polysilicon microgripper. In *Tech. Dig. IEEE Solid-State Sensor and Actuator Workshop*, pp. 48–51, Hilton Head, SC.

Lim, M. G.; Chang, J. C.; Schultz, D. P.; Howe, R. T.; White, R. M. (1990): Polysilicon microstructures to characterize static friction. In *Proc. IEEE Micro-Electro-Mechanical System Workshop*, pp. 9–14, Napa Vally, CA.

McMillan, J. A. (1993): *High frequency mechanical resonant devices*. Ph.D Thesis, Cornell University.

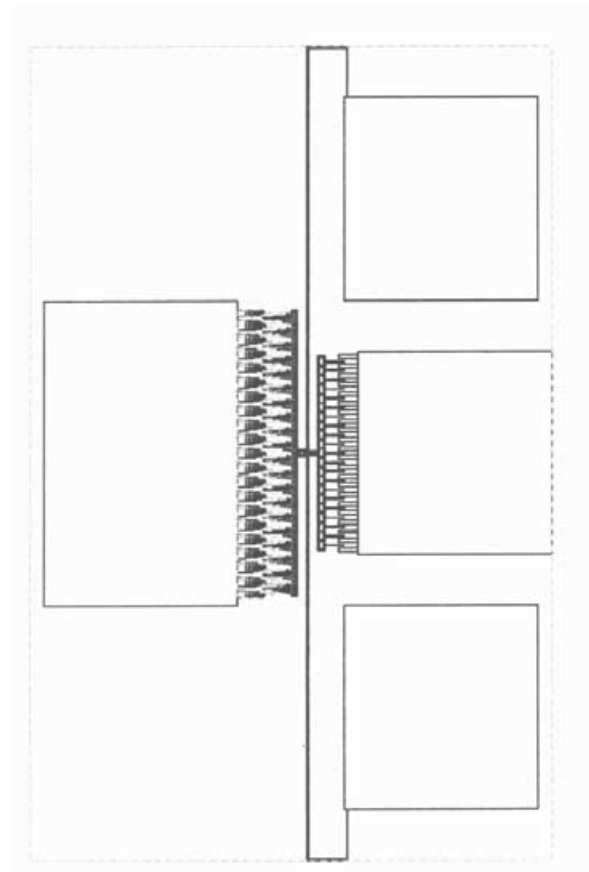


Figure 14 : CAD design of the device which contains one standard comb drive and one variable comb drive.

Pisano, A. P. (1989): Resonant-structure micromotors. In *Proc. IEEE Micro-Electro-Mechanical Systems Workshop*, pp. 1–8, Napa Vally, CA.

Senturia, S. D. (1995): CAD for microelectromechanical systems. In *Proc. the 8th International Conference on Solid-State Sensors and Actuators, and Eurosensors IX*, pp. 5–8, Stockholm, Sweden.

Shaw, K. A.; Zhang, Z. L.; MacDonald, N. C. (1994): Scream I: A single mask, single-crystal silicon, reactive ion etching process for microelectromechanical structures. *Sensors and Actuators A*, pp. 63–70.

Shi, F. (1995): *Simulation and analysis of micro-electro-mechanical systems with applications of sensitivity analysis and optimization*. Ph.D Thesis, Cornell University.

Shi, F.; Ramesh, P.; Mukherjee, S. (1995): On the application of 2D potential theory to electrostatic simulation. *Communications in Numerical Methods in Engineering*, pp. 691–701.

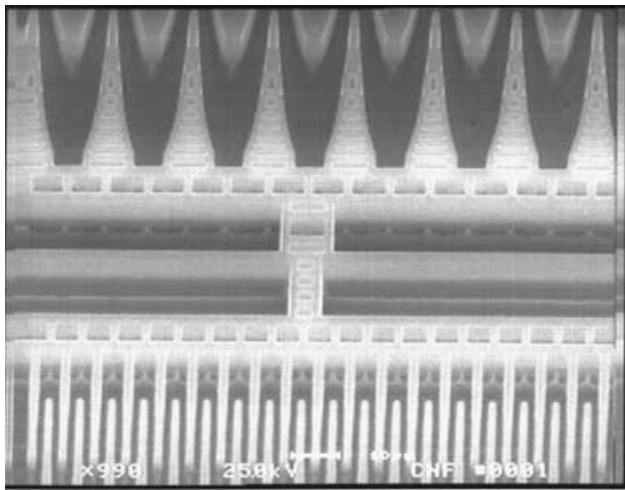


Figure 15 : SEM picture of part of the device after release.

Ye, W.; Mukherjee, S. (1999): Optimal shape design of three-dimensional MEMS with applications to electrostatic comb drives. *International Journal for Numerical Methods in Engineering*, pp. 175–194.

Ye, W.; Mukherjee, S.; MacDonald, N. (1998): Optimal shape design of an electrostatic comb drive in microelectromechanical systems. *Journal of Microelectromechanical Systems*, pp. 16–26.

Yun, W.; Howe, R. T.; Gray, P. R. (1992): Surface micromachined, digitally force-balanced accelerometer with integrated CMOS detection circuitry. In *Tech. Dig. IEEE Solid-State Sensor and Actuator Workshop*, pp. 126–131, Hilton Head, SC.